SPRIM: Structure-Preserving Reduced-Order Interconnect Macromodeling

Roland W. Freund
Department of Mathematics
University of California, Davis
One Shields Avenue
Davis, CA 95616, U.S.A.
freund@math.ucdavis.edu

ABSTRACT

In recent years, order-reduction techniques based on Krylov subspaces have become the methods of choice for generating macromodels of large multi-port RLC circuits. A widely-used method of this type is PRIMA. Its main features are provably passive reduced-order models and a moment-matching property. On the other hand, PRIMA does not preserve other structures, such as reciprocity or the block structure of the circuit matrices, inherent to RLC circuits, which makes it harder to synthesize the PRIMA models as actual circuits. Moreover, the PRIMA models match only half as many moments as optimal, but non-passive, moment-matching techniques such as SyMPVL. In this paper, we propose the new reduction technique SPRIM that overcomes these disadvantages of PRIMA. In particular, SPRIM generates provably passive and reciprocal macromodels of multi-port RLC circuits, and the SPRIM models match twice as many moments as the corresponding PRIMA models obtained with identical computational work. Numerical results are reported that illustrate the higher accuracy of SPRIM vs. PRIMA.

1. INTRODUCTION

Electronic circuits often contain large linear subnetworks of passive components. Such subnetworks may represent interconnect automatically extracted from layout as large RLC networks, models of IC packages, or models of wireless propagation channels. Often these subnetworks are so large that they need to be replaced by much smaller reduced-order models, before any numerical simulation becomes feasible. Ideally, these models would produce a good approximation of the input-output behavior of the original subnetwork, at least in a limited domain of interest, e.g., a frequency range.

*This research was performed while the author was with Bell Laboratories, Lucent Technologies.

In recent years, reduced-order modeling techniques based on Padé approximation have been recognized to be powerful tools for various circuit simulation tasks. The first such technique was asymptotic waveform evaluation (AWE) [21], which uses explicit moment matching. More recently, the attention has moved to reduced-order models generated by means of Krylov-subspace algorithms, which avoids the typical numerical instabilities of explicit moment matching.

PVL [8, 9] and its multi-port version MPVL [10] use variants of the Lanczos process [17] to stably compute reduced-order models that represent Padé or matrix-Padé approximations [5] of the circuit transfer function. SyPVL [14] and its multi-port version SyMPVL [11, 15, 16] are versions of PVL and MPVL, respectively, that are tailored to RLC circuits. By exploiting the symmetry of RLC transfer functions, the computational costs of SyPVL and SyMPVL are only half of those of general PVL and MPVL. The Arnoldi process [3] is another popular Krylov-subspace algorithm. Arnoldi-based reduced-order model techniques were recently proposed in [24, 19, 7, 20]. These models are not defined by Padé approximation, and as a result, in general, they are not as accurate as a Padé-based model of the same size. In fact, Arnoldi-based models are known to match only half as many moments as Lanczos-based models; see [24, 19, 20, 13].

In many applications, in particular those related to VLSI interconnect, the reduced-order model is used as a substitute for the full-blown original model in higher-level simulations. In such applications, it is very important for the reduced-order model to maintain the passivity properties of the original circuit. In [15, 16, 4], it is shown that SyMPVL is passive for RC, RL, and LC circuits. However, the Padé-based reduced-order model that characterizes SyMPVL cannot be guaranteed to be passive for general RLC circuits. On the other hand, in [19, 20], it was proved that the Arnoldi-based reduction technique PRIMA produces passive reduced-order for general RLC circuits. PRIMA employs a block version of the Arnoldi process and then obtains reduced-order models by projecting the matrices defining the RLC transfer function onto the Arnoldi basis vectors. While PRIMA generates provably passive reduced-order models, it does not preserve other structures, such as reciprocity or the block structure of the circuit matrices, inherent to RLC circuits. This has motivated the development of algorithms such as ENOR [23] and its variants [6] that generate passive and

reciprocal reduced-order models, yet still match as many moments as PRIMA. However, the moment-matching property of the PRIMA models is not optimal. In fact, the PRIMA models match only half as many moments as optimal, but non-passive, moment-matching techniques such as SyMPVL.

In this paper, we introduce the new reduction technique SPRIM that overcomes these disadvantages of PRIMA. In particular, SPRIM generates provably passive and reciprocal macromodels of multi-port RLC circuits, and the SPRIM models match twice as many moments as the corresponding PRIMA models obtained with identical computational work. Numerical results are reported that illustrate the higher accuracy of SPRIM vs. PRIMA.

2. RLC CIRCUIT EQUATIONS

In this section, we briefly review the form of RLC circuit equations.

The connectivity of a circuit can be captured using a directional graph. The nodes of the graph correspond to the nodes of the circuit, and the edges of the graph correspond to each of the circuit elements. An arbitrary direction is assigned to graph edges, so one can distinguish between the source and destination nodes. The adjacency matrix, $\mathbf{E}$, of the directional graph describes the connectivity of a circuit. Each row of $\mathbf{E}$ corresponds to a graph edge and, therefore, to a circuit element. Each column of $\mathbf{E}$ corresponds to a graph or circuit node. The column corresponding to the datum (ground) node of the circuit is omitted in order to remove redundancy. By convention, a row of $\mathbf{E}$ contains $+1$ in the column corresponding to the source node, -1 in the column corresponding to the destination node, and 0 everywhere else. Kirchhoff's laws, which depend only on connectivity, can be expressed in terms of $\mathbf{E}$ as follows:

$$\begin{aligned} \text{KCL:} \quad & \mathbf{E}^{\mathrm{T}}\,\mathbf{i}_b = \mathbf{0}, \\ \text{KVL:} \quad & \mathbf{E}\,\mathbf{v}_n = \mathbf{v}_b. \end{aligned} \tag{1}$$

Here, the vectors $\mathbf{i}_b$ and $\mathbf{v}_b$ contain the branch currents and voltages, respectively, and $\mathbf{v}_n$ the non-datum node voltages.

We are interested in analyzing RLC circuits, and for simplicity, we assume that the circuit is excited just by current sources. In this case, $\mathbf{E}$, $\mathbf{v}_b$, and $\mathbf{i}_b$ can be partitioned according to circuit-element types as follows:

$$\mathbf{E} = \begin{bmatrix} \mathbf{E}_i \\ \mathbf{E}_g \\ \mathbf{E}_c \\ \mathbf{E}_l \end{bmatrix}, \quad \mathbf{v}_b = \begin{bmatrix} \mathbf{v}_i \\ \mathbf{v}_g \\ \mathbf{v}_c \\ \mathbf{v}_l \end{bmatrix}, \quad \mathbf{i}_b = \begin{bmatrix} \mathbf{i}_i \\ \mathbf{i}_g \\ \mathbf{i}_c \\ \mathbf{i}_l \end{bmatrix}.$$

Here, the subscripts i, g, c, and l stand for branches containing current sources, resistors, capacitors, and inductors, respectively.

The set of circuit equations is completed by adding the so-called *branch constitutive relationships* (BCRs), which describe the physical behavior of the circuit elements. In the case of RLC circuits, the BCRs are as follows:

$$\mathbf{i}_i = -\mathbf{I}_t(t),\ \mathbf{i}_g = \mathbf{G}\,\mathbf{v}_g,\ \mathbf{i}_c = \mathbf{C}\,\frac{d}{dt}\mathbf{v}_c,\ \mathbf{v}_l = \mathbf{L}\,\frac{d}{dt}\mathbf{i}_l. \tag{2}$$

Here, $\mathbf{I}_t(t)$ is the vector of current-source values, $\mathbf{G}$ and $\mathbf{C}$ are diagonal matrices whose diagonal entries are the conductance and capacitance values of each element. Clearly, these values are positive for any physical circuit. The inductance matrix $\mathbf{L}$ is always symmetric and positive semi-definite. In the absence of inductive coupling, $\mathbf{L}$ is also a diagonal matrix. However, in the case of inductive coupling, the matrix $\mathbf{L}$ is full in general. An important special case is inductance matrix $\mathbf{L}$ whose inverse, the so-called susceptance matrix, $\mathbf{S} = \mathbf{L}^{-1}$ is sparse; see [27, 28].

The modified nodal formulation (MNA) of the circuit equations is obtained by combining equations (1) with (2), and eliminating as many current unknowns as possible. For RLC circuits, only inductor currents are left as unknowns. The resulting MNA equations are

$$\begin{gathered} \mathcal{G}\,\mathbf{x} + \mathcal{C}\,\frac{d}{dt}\mathbf{x} = \mathcal{B}\,\mathbf{I}_t(t), \\ \text{where} \quad \mathcal{G} = \begin{bmatrix} \mathbf{E}_g^{\mathrm{T}}\mathbf{G}\,\mathbf{E}_g & \mathbf{E}_l^{\mathrm{T}} \\ -\mathbf{E}_l & \mathbf{0} \end{bmatrix}, \quad \mathbf{x} = \begin{bmatrix} \mathbf{v}_n \\ \mathbf{i}_l \end{bmatrix}, \\ \mathcal{C} = \begin{bmatrix} \mathbf{E}_c^{\mathrm{T}}\mathbf{C}\,\mathbf{E}_c & \mathbf{0} \\ \mathbf{0} & \mathbf{L} \end{bmatrix}, \quad \mathcal{B} = \begin{bmatrix} \mathbf{E}_i^{\mathrm{T}} \\ \mathbf{0} \end{bmatrix}. \end{gathered} \tag{3}$$

We remark that $\mathbf{G}$, $\mathbf{C}$, and $\mathbf{L}$ are symmetric positive definite matrices. This implies that

$$\mathcal{G} + \mathcal{G}^{\mathrm{T}} \succeq \mathbf{0} \quad \text{and} \quad \mathcal{C} \succeq \mathbf{0}. \tag{4}$$

Here, $\mathcal{M} \succeq \mathbf{0}$ means that the matrix $\mathcal{M}$ is symmetric and positive semi-definite.

We view the RLC circuit as an m-terminal component, and next, we determine its network functions. Since we allowed only current sources, it is natural to determine the matrix $\mathbf{Z}(s)$ of $\mathbf{Z}$-parameters. By applying the Laplace transform to (3) and assuming zero initial conditions, we obtain

$$\begin{aligned} (\mathcal{G} + s\,\mathcal{C})\,\mathbf{X} &= \mathcal{B}\,\mathbf{I}_s(s), \\ \mathbf{V}_i &= \mathcal{B}^{\mathrm{T}}\,\mathbf{X}. \end{aligned} \tag{5}$$

Here, $\mathbf{X}$, $\mathbf{I}_s(s)$, and $\mathbf{V}_i$ represent the Laplace transforms of the unknown vector $\mathbf{x}$, the excitation current $\mathbf{I}_t(t)$, and the vector of voltages across the excitation sources, respectively. Eliminating $\mathbf{X}$ in (5) gives

$$\begin{gathered} \mathbf{V}_i = \begin{bmatrix} \mathbf{E}_i & \mathbf{0} \end{bmatrix} \mathbf{X} = \mathbf{Z}(s)\,\mathbf{I}_s(s), \\ \text{where} \quad \mathbf{Z}(s) = \mathcal{B}^{\mathrm{T}}\,(\mathcal{G} + s\,\mathcal{C})^{-1}\,\mathcal{B}. \end{gathered} \tag{6}$$

3. ORDER REDUCTION BY PROJECTION

In this section, we discuss reduced-order modeling via one-sided projection onto block Krylov subspaces.

We consider general m-input m-output transfer functions of the form

$$\mathbf{Z}(s) = \mathcal{B}^{\mathrm{T}}\,(\mathcal{G} + s\,\mathcal{C})^{-1}\,\mathcal{B}, \tag{7}$$

where the matrices $\mathcal{G}$ and $\mathcal{C}$ are $N \times N$, and $\mathcal{B}$ is $N \times m$. We remark that N is called the state-space dimension of (7). Moreover, we assume that $\mathcal{G}$, $\mathcal{C}$, and $\mathcal{B}$ have the block structure

$$\mathcal{G} = \begin{bmatrix} \mathbf{G}_1 & \mathbf{G}_2^{\mathrm{T}} \\ -\mathbf{G}_2 & \mathbf{0} \end{bmatrix}, \quad \mathcal{C} = \begin{bmatrix} \mathbf{C}_1 & \mathbf{0} \\ \mathbf{0} & \mathbf{C}_2 \end{bmatrix}, \quad \mathcal{B} = \begin{bmatrix} \mathbf{B}_1 \\ \mathbf{0} \end{bmatrix}, \tag{8}$$

where the subblocks $\mathbf{G}_1$, $\mathbf{C}_1$, and $\mathbf{B}_1$ have the same number of rows, and

$$\mathbf{G}_1 \succeq \mathbf{0}, \quad \mathbf{C}_1 \succeq \mathbf{0}, \quad \mathbf{C}_2 \succ \mathbf{0}. \tag{9}$$

The conditions (9) imply that the matrices $\mathcal{G}$ and $\mathcal{C}$ satisfy (4). We also assume that $\mathcal{G} + s\,\mathcal{C}$ is a regular matrix pencil, i.e., the matrix $\mathcal{G} + s\,\mathcal{C}$ is singular only for finitely many values of $s \in \mathbb{C}$. Clearly, RLC transfer functions of the form (6) are a special case of (7).

3.1 Reduced-Order Models

Let $n\,(< N)$ denote the desired state-space dimension of a reduced-order model of the original transfer function (7), $\mathbf{Z}$, of state-space dimension N.

A reduced-order model of state-space dimension n is given by a reduced-order transfer function $\mathbf{Z}_n$ of the form

$$\mathbf{Z}_n(s) = \mathcal{B}_n^{\mathrm{T}}\,(\mathcal{G}_n + s\,\mathcal{C}_n)^{-1}\,\mathcal{B}_n \tag{10}$$

where $\mathcal{G}_n$ and $\mathcal{C}_n$ are $n \times n$ matrices, and $\mathcal{B}_n$ is an $n \times m$ matrix. Note that, in order for (10) to be meaningful, the matrix pencil $\mathcal{G}_n + s\,\mathcal{C}_n$ needs to be regular.

Reduced-order models (10) can be obtained easily by means of projection. To this end, let

$$\mathcal{V}_n = \begin{bmatrix} \mathbf{v}_1 & \mathbf{v}_2 & \cdots & \mathbf{v}_n \end{bmatrix} \tag{11}$$

be any $N \times n$ matrix, and set

$$\mathcal{G}_n = \mathcal{V}_n^{\mathrm{T}}\,\mathcal{G}\,\mathcal{V}_n, \quad \mathcal{C}_n = \mathcal{V}_n^{\mathrm{T}}\,\mathcal{C}\,\mathcal{V}_n, \quad \mathcal{B}_n = \mathcal{V}_n^{\mathrm{T}}\,\mathcal{B}. \tag{12}$$

Provided that the matrix $\mathcal{V}_n$ is such that the matrix pencil $\mathcal{G}_n + s\,\mathcal{C}_n$ is regular, the matrices (12) define a reduced-order model.

3.2 Block Krylov Subspaces

The simple projection (12) yields powerful model-order reduction techniques, such as SyMPVL and PRIMA, when the columns of the matrix (11), $\mathcal{V}_n$, are chosen as basis vector of certain block Krylov subspaces.

To this end, let $s_0 \in \mathbb{C}$ be a suitably chosen expansion point such that the matrix $\mathcal{G} + s_0\,\mathcal{C}$ is nonsingular. We can then rewrite (7) as follows:

$$\begin{aligned} \mathbf{Z}(s) &= \mathcal{B}^{\mathrm{T}}\,(\mathcal{G} + s_0\,\mathcal{C} + (s - s_0)\,\mathcal{C})^{-1}\,\mathcal{B} \\ &= \mathcal{B}^{\mathrm{T}}\,(\mathcal{I} + (s - s_0)\,\mathcal{A})^{-1}\,\mathcal{R}, \end{aligned} \tag{13}$$

$$\text{where} \quad \mathcal{A} = (\mathcal{G} + s_0\,\mathcal{C})^{-1}\,\mathcal{C}, \quad \mathcal{R} = (\mathcal{G} + s_0\,\mathcal{C})^{-1}\,\mathcal{B}.$$

We will use block Krylov subspaces induced by the matrices $\mathcal{A}$ and $\mathcal{R}$ in (13) to generate reduced-order models for (7). Next, we briefly review the notion of block Krylov subspaces; see [1] for a more detailed discussion. The matrix sequence $\mathcal{R}, \mathcal{A}\,\mathcal{R}, \mathcal{A}^2\,\mathcal{R}, \ldots, \mathcal{A}^{q-1}\,\mathcal{R}, \ldots$ is called a *block Krylov sequence*. The columns of the matrices in this sequence are vectors of length N, and thus at most N of these columns are linearly independent. By scanning the columns of the matrices in the block Krylov sequence from left to right and deleting each column that is linearly dependent on earlier columns, we obtain the *deflated* block Krylov sequence

$$\mathcal{R}_1, \mathcal{A}\,\mathcal{R}_2, \mathcal{A}^2\,\mathcal{R}_3, \ldots, \mathcal{A}^{q_{\max}-1}\,\mathcal{R}_{q_{\max}}. \tag{14}$$

This process of deleting linearly dependent vectors is called *deflation*. In (14), each $\mathcal{R}_q$ is a submatrix of $\mathcal{R}_{q-1}$. Denoting by m_q the number of columns of $\mathcal{R}_q$, we thus have

$$m \geq m_1 \geq m_2 \geq \cdots \geq m_{q_{\max}} \geq 1. \tag{15}$$

By construction, the columns of the matrices (14) are linearly independent, and for each n, the subspace spanned by the first n of these columns is called the *n-th block Krylov subspace* (induced by $\mathcal{A}$ and $\mathcal{R}$) and denoted by $\mathcal{K}_n(\mathcal{A}, \mathcal{R})$ in the sequel.

In the following, we always assume that $1 \leq q \leq q_{\max}$ is arbitrary, and we set

$$n = m_1 + m_2 + \cdots + m_q. \tag{16}$$

Note that, by (15), $n \leq m \cdot q$ with $n = m \cdot q$ if no deflation has occurred. For n in (16), the n-th block Krylov subspace is given by

$$\mathcal{K}_n(\mathcal{A}, \mathcal{R}) = \mathrm{colspan}\{\mathcal{R}_1, \mathcal{A}\,\mathcal{R}_2, \ldots, \mathcal{A}^{q-1}\,\mathcal{R}_q\}.$$

3.3 PRIMA and Moment Matching

PRIMA combines projection with block Krylov subspaces. More precisely, the n-th PRIMA model $\mathbf{Z}_n$ is defined by (10) and (12), where the matrix (11), $\mathcal{V}_n$, is chosen such that its columns span the n-th block Krylov subspace $\mathcal{K}_n(\mathcal{A}, \mathcal{R})$, i.e.,

$$\mathrm{span}\,\mathcal{V}_n = \mathcal{K}_n(\mathcal{A}, \mathcal{R}). \tag{17}$$

Although the PRIMA model $\mathbf{Z}_n$ is defined by a simple projection, $\mathbf{Z}_n$ satisfies a moment-matching property. For the special case $s_0 = 0$ and basis vectors generated by block Arnoldi without deflation, the moment-matching property was first observed in [19]. In [12], this result was extended to the most general case where possibly nonzero expansion points s_0 are allowed and where the underlying block Krylov subspaces allow the necessary deflation of linearly dependent vectors. The result can be stated as follows.

THEOREM 1. *Let $n = m_1 + m_2 + \cdots + m_q$ and the matrix $\mathcal{V}_n$ in (11) satisfy (17). Then, the first q moments in the expansions of $\mathbf{Z}$ and the n-th PRIMA model $\mathbf{Z}_n$ about s_0 are identical*:

$$\mathbf{Z}(s) = \mathbf{Z}_n(s) + \mathcal{O}\left((s - s_0)^q\right).$$

Recall that, for RLC circuits, the matrices $\mathcal{G}$, $\mathcal{C}$, and $\mathcal{B}$ in (7) exhibit the particular block structure (8). However, for the PRIMA reduced-order model, the matrices $\mathcal{G}_n$, $\mathcal{C}_n$, and $\mathcal{B}_n$ in (10) and (12) are dense in general, and in particular, the block structure (8) is not preserved.

Next, we describe the SPRIM reduction technique, which preserves the block structure (8) and at the same time, matches twice as many moments ar PRIMA.

4. THE SPRIM ALGORITHM

The development of the SPRIM algorithm was motivated by the following insight. In order to have the moment-matching property stated in Theorem 1, it is not necessary that the projection matrix $\mathcal{V}_n$ satisfies (17). Instead, let $\widetilde{\mathcal{V}}_n$ be any matrix, possibly with more than n columns, such that the

space spanned by the columns of $\widetilde{\mathcal{V}}_n$ contains the n-th block Krylov subspace $\mathcal{K}_n(\mathcal{A},\mathcal{R})$, i.e.,

$$\mathcal{K}_n(\mathcal{A},\mathcal{R}) \subseteq \operatorname{span} \widetilde{\mathcal{V}}_n. \tag{18}$$

Then, using such a matrix $\widetilde{\mathcal{V}}_n$, we define a reduced-order model as follows:

$$\widetilde{\mathbf{Z}}_n(s) = \widetilde{\mathcal{B}}_n^{\mathrm{T}} \left(\widetilde{\mathcal{G}}_n + s\,\widetilde{\mathcal{C}}_n\right)^{-1} \widetilde{\mathcal{B}}_n, \tag{19}$$

where

$$\widetilde{\mathcal{G}}_n = \widetilde{\mathcal{V}}_n^{\mathrm{T}}\,\mathcal{G}\,\widetilde{\mathcal{V}}_n, \quad \widetilde{\mathcal{C}}_n = \widetilde{\mathcal{V}}_n^{\mathrm{T}}\,\mathcal{C}\,\widetilde{\mathcal{V}}_n, \quad \widetilde{\mathcal{B}}_n = \widetilde{\mathcal{V}}_n^{\mathrm{T}}\,\mathcal{B}. \tag{20}$$

In analogy to Theorem 1, we have the following result.

THEOREM 2. *Let $n = m_1 + m_2 + \cdots + m_q$ and let $\widetilde{\mathcal{V}}_n$ be a matrix, possibly with more than n columns, such that* (18) *is satisfied. Then, the first q moments in the expansions of $\mathbf{Z}$ and the projected model $\widetilde{\mathbf{Z}}_n$ (defined by* (19) *and* (20)*) about s_0 are identical*:

$$\mathbf{Z}(s) = \widetilde{\mathbf{Z}}_n(s) + \mathcal{O}\left((s-s_0)^q\right).$$

PROOF. It is easy to see that the proof of [13, Theorem 7] readily extends to the slightly more general situation of Theorem 2. □

Now let $\mathcal{V}_n$ again be the basis matrix used in PRIMA. Recall that $\mathcal{V}_n$ satisfies (17). Let

$$\mathcal{V}_n = \begin{bmatrix} \mathbf{V}_1 \\ \mathbf{V}_2 \end{bmatrix}$$

be the partitioning of $\mathcal{V}_n$ corresponding to the block sizes of $\mathcal{G}$ and $\mathcal{C}$ in (8). We set

$$\widetilde{\mathcal{V}}_n = \begin{bmatrix} \mathbf{V}_1 & \mathbf{0} \\ \mathbf{0} & \mathbf{V}_2 \end{bmatrix}. \tag{21}$$

Together with (17), it follows that

$$\mathcal{K}_n(\mathcal{A},\mathcal{R}) = \operatorname{span} \mathcal{V}_n \subseteq \operatorname{span} \widetilde{\mathcal{V}}_n.$$

Hence, we can project onto the columns of $\widetilde{\mathcal{V}}_n$, and in view of Theorem 2, we obtain a reduced-order model that matches at least as many moments as PRIMA. In fact, as we will show in the next section, the resulting SPRIM reduced-order model even matches twice as many moments as PRIMA. Furthermore, the special block structure (21) of the matrix $\widetilde{\mathcal{V}}_n$ implies that the SPRIM reduced-order model $\widetilde{\mathbf{Z}}_n$ preserves the block structure (8) of the original transfer function $\mathbf{Z}$.

An outline of the SPRIM algorithm is as follows.

SPRIM algorithm:

- Input: matrices

  $$\mathcal{G} = \begin{bmatrix} \mathbf{G}_1 & \mathbf{G}_2^{\mathrm{T}} \\ -\mathbf{G}_2 & \mathbf{0} \end{bmatrix}, \quad \mathcal{C} = \begin{bmatrix} \mathbf{C}_1 & \mathbf{0} \\ \mathbf{0} & \mathbf{C}_2 \end{bmatrix}, \quad \mathcal{B} = \begin{bmatrix} \mathbf{B}_1 \\ \mathbf{0} \end{bmatrix},$$

  where the subblocks $\mathbf{G}_1$, $\mathbf{C}_1$, and $\mathbf{B}_1$ have the same number of rows, and the subblocks of $\mathcal{G}$ and $\mathcal{C}$ satisfy $\mathbf{G}_1 \succeq \mathbf{0}$, $\mathbf{C}_1 \succeq \mathbf{0}$, and $\mathbf{C}_2 \succ \mathbf{0}$;
  an expansion point s_0.

- Formally set

  $$\mathcal{A} = (\mathcal{G} + s_0\,\mathcal{C})^{-1}\,\mathcal{C}, \quad \mathcal{R} = (\mathcal{G} + s_0\,\mathcal{C})^{-1}\,\mathcal{B}.$$

- Until n is large enough, run your favorite block Krylov subspace method (applied to $\mathcal{A}$ and $\mathcal{R}$) to construct the columns of the basis matrix

  $$\mathcal{V}_n = \begin{bmatrix} \mathbf{v}_1 & \mathbf{v}_2 & \cdots & \mathbf{v}_n \end{bmatrix}$$

  of the n-th block Krylov subspace $\mathcal{K}_n(\mathcal{A},\mathcal{R})$, i.e.,

  $$\operatorname{span} \mathcal{V}_n = \mathcal{K}_n(\mathcal{A},\mathcal{R}).$$

- Let

  $$\mathcal{V}_n = \begin{bmatrix} \mathbf{V}_1 \\ \mathbf{V}_2 \end{bmatrix}$$

  be the partitioning of $\mathcal{V}_n$ corresponding to the block sizes of $\mathcal{G}$ and $\mathcal{C}$.

- Set

  $$\begin{aligned} \widetilde{\mathbf{G}}_1 &= \mathbf{V}_1^{\mathrm{T}}\,\mathbf{G}_1\,\mathbf{V}_1, \quad \widetilde{\mathbf{G}}_2 = \mathbf{V}_2^{\mathrm{T}}\,\mathbf{G}_2\,\mathbf{V}_1, \\ \widetilde{\mathbf{C}}_1 &= \mathbf{V}_1^{\mathrm{T}}\,\mathbf{C}_1\,\mathbf{V}_1, \quad \widetilde{\mathbf{C}}_2 = \mathbf{V}_2^{\mathrm{T}}\,\mathbf{C}_2\,\mathbf{V}_2, \\ \widetilde{\mathbf{B}}_1 &= \mathbf{V}_1^{\mathrm{T}}\,\mathbf{B}_1 \end{aligned}$$

  and

  $$\begin{aligned} \widetilde{\mathcal{G}}_n &= \begin{bmatrix} \widetilde{\mathbf{G}}_1 & \widetilde{\mathbf{G}}_2^{\mathrm{T}} \\ -\widetilde{\mathbf{G}}_2 & \mathbf{0} \end{bmatrix}, \quad \widetilde{\mathcal{C}}_n = \begin{bmatrix} \widetilde{\mathbf{C}}_1 & \mathbf{0} \\ \mathbf{0} & \widetilde{\mathbf{C}}_2 \end{bmatrix}, \\ \widetilde{\mathcal{B}}_n &= \begin{bmatrix} \widetilde{\mathbf{B}}_1 \\ \mathbf{0} \end{bmatrix}. \end{aligned} \tag{22}$$

- Output: the reduced-order model $\widetilde{\mathbf{Z}}_n$ in first-order form

  $$\widetilde{\mathbf{Z}}_n(s) = \widetilde{\mathcal{B}}_n^{\mathrm{T}} \left(\widetilde{\mathcal{G}}_n + s\,\widetilde{\mathcal{C}}_n\right)^{-1} \widetilde{\mathcal{B}}_n, \tag{23}$$

  and in second-order form

  $$\widetilde{\mathbf{Z}}_n(s) = \widetilde{\mathbf{B}}_1^{\mathrm{T}} \left(s\,\widetilde{\mathbf{C}}_1 + \widetilde{\mathbf{G}}_1 + \frac{1}{s}\widetilde{\mathbf{G}}_2^{\mathrm{T}}\,\widetilde{\mathbf{C}}_2^{-1}\,\widetilde{\mathbf{G}}_2\right)^{-1} \widetilde{\mathbf{B}}_1. \tag{24}$$

We remark that the main computational cost of the SPRIM algorithm is running the block Krylov subspace method to obtain $\mathcal{V}_n$. This is the same as for PRIMA. Thus generating the PRIMA reduced-order model $\mathbf{Z}_n$ and the SPRIM reduced-order model $\widetilde{\mathbf{Z}}_n$ involves the same computational costs.

On the other hand, when written in first-order form (23), it would appear that the SPRIM model has state-space dimension $2n$, and thus it would be twice as large as the corresponding PRIMA model. However, unlike the PRIMA model, the SPRIM model can always be represented in the second-order form (24); see Subsection 5.3 below. In (24), the matrices $\widetilde{\mathbf{C}}_1$, $\widetilde{\mathbf{G}}_1$, and $\widetilde{\mathbf{G}}_2^{\mathrm{T}}\,\widetilde{\mathbf{C}}_2^{-1}\,\widetilde{\mathbf{G}}_2$ are all of size $n \times n$, and the matrix $\widetilde{\mathbf{B}}_1$ is of size $n \times m$. These are the same dimensions as in the PRIMA mdoel (10). Therefore, the SPRIM model $\widetilde{\mathbf{Z}}_n$ (written in second-order form (24)) and of the corresponding PRIMA model $\mathbf{Z}_n$ indeed have the same state-space dimension n.

5. PROPERTIES OF SPRIM

In this section, we describe some properties of the SPRIM algorithm.

5.1 Moment Matching

Recall that, in view of Theorem 2, the SPRIM reduced-order model matches at least as many moments as the PRIMA reduced-order model. However, it turns out that the SPRIM model matches even twice as many moments, at least as long as the expansion point s_0 is chosen to be a real number, i.e., $s_0 \in \mathbb{R}$. Note that, in practice, in order to avoid complex arithmetic, one usually chooses $s_0 \in \mathbb{R}$ anyway.

This enhanced moment-matching property can be stated as follows.

THEOREM 3. *Let $s_0 \in \mathbb{R}$. Let $n = m_1 + m_2 + \cdots + m_q$ and let $\widetilde{\mathcal{V}}_n$ be the matrix (21) that is used in the SPRIM algorithm. Then, the first $2q$ moments in the expansions of $\mathbf{Z}$ and the projected model $\widetilde{\mathbf{Z}}_n$ (defined by (19) and (20)) about s_0 are identical:*

$$\mathbf{Z}(s) = \widetilde{\mathbf{Z}}_n(s) + \mathcal{O}\left((s - s_0)^{2q}\right).$$

We remark that for the special case of $s_0 = 0$, the result of this theorem can be traced back to [25]. Next, we present the proof of Theorem 3 for the general case of $s_0 \in \mathbb{R}$.

PROOF. First, note that from (13), we obtain the expansion

$$\mathbf{Z}(s) = \sum_{j=0}^{\infty} (-1)^j \, \mathcal{B}^{\mathrm{T}} \, \mathcal{A}^j \, \mathcal{R} \, (s - s_0)^j. \tag{25}$$

Similarly, using the first-order representation (23) of $\widetilde{\mathbf{Z}}_n$, we have

$$\widetilde{\mathbf{Z}}_n(s) = \sum_{j=0}^{\infty} (-1)^j \, \widetilde{\mathcal{B}}_n^{\mathrm{T}} \, \widetilde{\mathcal{A}}_n^j \, \widetilde{\mathcal{R}}_n \, (s - s_0)^j, \tag{26}$$

where

$$\widetilde{\mathcal{A}}_n = \left(\widetilde{\mathcal{G}}_n + s_0 \, \widetilde{\mathcal{C}}_n\right)^{-1} \widetilde{\mathcal{C}}_n, \quad \widetilde{\mathcal{R}}_n = \left(\widetilde{\mathcal{G}}_n + s_0 \, \widetilde{\mathcal{C}}_n\right)^{-1} \widetilde{\mathcal{B}}_n. \tag{27}$$

In view of (25) and (26), the claim of Theorem 3 is equivalent to the following property:

$$\mathcal{B}^{\mathrm{T}} \, \mathcal{A}^j \, \mathcal{R} = \widetilde{\mathcal{B}}_n^{\mathrm{T}} \, \widetilde{\mathcal{A}}_n^j \, \widetilde{\mathcal{R}}_n, \quad j = 0, 1, \ldots, 2q - 1. \tag{28}$$

We prove (28) by establishing these relations:

$$\mathcal{B}^{\mathrm{T}} \, \mathcal{A}^{j_1} \, \widetilde{\mathcal{V}}_n = \widetilde{\mathcal{B}}_n^{\mathrm{T}} \, \widetilde{\mathcal{A}}_n^{j_1}, \quad j_1 = 0, 1, \ldots, q, \tag{29}$$

and

$$\mathcal{A}^{j_2} \, \mathcal{R} = \widetilde{\mathcal{V}}_n \, \widetilde{\mathcal{A}}_n^{j_2} \, \widetilde{\mathcal{R}}_n, \quad j_2 = 0, 1, \ldots, q - 1. \tag{30}$$

Indeed, (29) and (30) together imply

$$\begin{aligned} \mathcal{B}^{\mathrm{T}} \, \mathcal{A}^{j_1 + j_2} \, \mathcal{R} &= \mathcal{B}^{\mathrm{T}} \, \mathcal{A}^{j_1} \, \widetilde{\mathcal{V}}_n \, \widetilde{\mathcal{A}}_n^{j_2} \, \widetilde{\mathcal{R}}_n \\ &= \widetilde{\mathcal{B}}_n^{\mathrm{T}} \, \widetilde{\mathcal{A}}_n^{j_1 + j_2} \, \widetilde{\mathcal{R}}_n, \quad j_1 + j_2 = 0, 1, \ldots, 2q - 1, \end{aligned}$$

which is just the desired identity (28).

Thus it remains to show (29) and (30). The relation (30) is essentially the one established in [13, Proposition 6], and we refer the reader to the proof in that paper. We stress that the relation (30) holds true for general transfer functions (7), and that it does not require the special structures (8) or (9). The relation (29), on the other hand, follows from (30) and the special structures (8) and (9).

A sketch of the proof of (29) is as follows. Since $\widetilde{\mathcal{B}}_n = \widetilde{\mathcal{V}}_n^{\mathrm{T}} \, \mathcal{B}$, (29) is trivially satisfied for $j_1 = 0$. Therefore, let $1 \leq j_1 \leq q$. Using (8) and (9) one readily verifies that

$$\left(\mathcal{A}^{\mathrm{T}}\right)^{j_1} = \mathcal{J}^{-1} \left(\mathcal{C} \left(\mathcal{G} + s_0 \, \mathcal{C}\right)^{-1}\right)^{j_1} \mathcal{J} \quad \text{and} \quad \mathcal{B} = \mathcal{J} \, \mathcal{B}, \tag{31}$$

where

$$\mathcal{J} = \mathcal{J}^{-1} = \begin{bmatrix} \mathbf{I}_1 & \mathbf{0} \\ \mathbf{0} & -\mathbf{I}_2 \end{bmatrix}$$

and $\mathbf{J}_1$ and $\mathbf{J}_2$ are identity matrices of the size of the diagonal blocks of $\mathcal{G}$ and $\mathcal{C}$. Since the matrices $\widetilde{\mathcal{G}}_n$ and $\widetilde{\mathcal{C}}_n$ exhibit the same structures as $\mathcal{G}$ and $\mathcal{C}$, we also have the relation

$$\left(\widetilde{\mathcal{A}}_n^{\mathrm{T}}\right)^{j_1} = \mathcal{J}_n^{-1} \left(\widetilde{\mathcal{C}}_n \left(\widetilde{\mathcal{G}}_n + s_0 \, \widetilde{\mathcal{C}}_n\right)^{-1}\right)^{j_1} \mathcal{J}_n, \tag{32}$$

where $\mathcal{J}_n$ is the appropriate reduced-oder version of $\mathcal{J}$. Recall that $\mathcal{R} = \left(\mathcal{G} + s_0 \, \mathcal{C}\right)^{-1} \mathcal{B}$, and together with (31), it follows that

$$\left(\mathcal{A}^{\mathrm{T}}\right)^{j_1} \mathbf{B} = \mathcal{J}^{-1} \, \mathcal{C} \, \mathcal{A}^{j_1 - 1} \mathcal{R}. \tag{33}$$

Inserting the relation (30) (with $j_2 = j_1 - 1$) into (33), we get

$$\begin{aligned} \left(\mathcal{A}^{\mathrm{T}}\right)^{j_1} \mathbf{B} &= \mathcal{J}^{-1} \, \mathcal{C} \, \widetilde{\mathcal{V}}_n^{\mathrm{T}} \, \widetilde{\mathcal{A}}_n^{j_1 - 1} \widetilde{\mathcal{R}}_n \\ &= \mathcal{J}^{-1} \, \mathcal{C} \, \widetilde{\mathcal{V}}_n^{\mathrm{T}} \, \widetilde{\mathcal{A}}_n^{j_1 - 1} \left(\widetilde{\mathcal{G}}_n + s_0 \, \widetilde{\mathcal{C}}_n\right)^{-1} \widetilde{\mathcal{B}}_n. \end{aligned} \tag{34}$$

By taking the transpose of (34), multiplying the result from the right by $\widetilde{\mathcal{V}}_n$, and using (32), one readily verifies that

$$\begin{aligned} \mathcal{B}^{\mathrm{T}} \, \mathcal{A}^{j_1} \, \widetilde{\mathcal{V}}_n &= \widetilde{\mathcal{B}}_n^{\mathrm{T}} \, \widetilde{\mathcal{A}}_n^{j_1 - 1} \, \mathcal{J}_n \left(\widetilde{\mathcal{C}}_n (\widetilde{\mathcal{G}}_n + s_0 \, \widetilde{\mathcal{C}}_n)^{-1}\right)^{\mathrm{T}} \mathcal{J}_n \\ &= \widetilde{\mathcal{B}}_n^{\mathrm{T}} \, \widetilde{\mathcal{A}}_n^{j_1}. \end{aligned}$$

This is just the desired relation (29), and the proof is complete. □

5.2 Passivity

We now return to the RLC transfer functions $\mathbf{Z}$ described in Section 2. Recall that $\mathbf{Z}$ is defined by (6) with $\mathcal{G}$, $\mathcal{C}$, $\mathcal{B}$ given by (3). In this subsection, we assume that $s_0 \in \mathbb{R}$.

It is well known (see, e.g., [2, 26]) that $\mathbf{Z}$ is *passive* if, and only if, the following three conditions are satisfied:

(i) $\mathbf{Z}(s)$ has no poles in $\mathbb{C}_+ = \{ s \in \mathbb{C} \mid \mathrm{Re}\, s > 0 \}$;

(ii) $\mathbf{Z}(\bar{s}) = \overline{\mathbf{Z}(s)}$ for all $s \in \mathbb{C}$;

(iii) $\mathrm{Re}\left(\mathbf{x}^{\mathrm{H}} \, \mathbf{Z}(s) \, \mathbf{x}\right) \geq 0$ for all $s \in \mathbb{C}_+$ and $\mathbf{x} \in \mathbb{C}^m$.

In particular, RLC transfer functions $\mathbf{Z}$ are passive.

In [12, 13], it was shown that reduced-order models of RLC circuits obtained by projection, as described in Section 3, preserve passivity. In particular, this result applies to the SPRIM model, and so we have the following theorem.

THEOREM 4. *The SPRIM reduced-order model* $\widetilde{\mathbf{Z}}_n$ *given by* (23) (*or, equivalently,* (24)) *is passive.*

5.3 Second-Order Form

The original transfer function (7) can be rewritten in so-called second-order form.

Indeed, using the block structure (8), it is easy to verify that the matrix $(\mathcal{G}+s\,\mathcal{C})^{-1}$ in (7) is of the form

$$(\mathcal{G}+s\,\mathcal{C})^{-1} = \begin{bmatrix} (\mathbf{Q}(s))^{-1} & \star \\ \star & \star \end{bmatrix}, \tag{35}$$

where

$$\mathbf{Q}(s) = s\,\mathbf{C}_1 + \mathbf{G}_1 + \frac{1}{s}\mathbf{G}_2^{\mathrm{T}}\,\mathbf{C}_2^{-1}\,\mathbf{G}_2. \tag{36}$$

Inserting (35) into (7), it follows that the transfer function $\mathbf{Z}$ can also be rewritten as follows:

$$\mathbf{Z}(s) = \mathbf{B}_1^{\mathrm{T}}\left(s\,\mathbf{C}_1 + \mathbf{G}_1 + \frac{1}{s}\mathbf{G}_2^{\mathrm{T}}\,\mathbf{C}_2^{-1}\,\mathbf{G}_2\right)^{-1}\mathbf{B}_1. \tag{37}$$

Moreover, in view of (9), the coefficient matrices of $\mathbf{Q}$ in (36) satisfy

$$\mathbf{C}_1 \succeq \mathbf{0}, \quad \mathbf{G}_1 \succeq \mathbf{0}, \quad \mathbf{G}_2^{\mathrm{T}}\,\mathbf{C}_2^{-1}\,\mathbf{G}_2 \succeq \mathbf{0},$$

and thus they are in particular symmetric. This means that the transfer function (37), $\mathbf{Z}$, is reciprocal; see, e.g., [2].

Since PRIMA does not preserve the block structure (8) of the original transfer function, the PRIMA model cannot be written in second-order form and is not reciprocal in general. The SPRIM model $\widetilde{\mathbf{Z}}_n$ however, can always be written in second-order form. Indeed, using (22) and (23), it follows that

$$\widetilde{\mathbf{Z}}_n(s) = \widetilde{\mathbf{B}}_1^{\mathrm{T}}\left(s\,\widetilde{\mathbf{C}}_1 + \widetilde{\mathbf{G}}_1 + \frac{1}{s}\widetilde{\mathbf{G}}_2^{\mathrm{T}}\,\widetilde{\mathbf{C}}_2^{-1}\,\widetilde{\mathbf{G}}_2\right)^{-1}\widetilde{\mathbf{B}}_1,$$

and

$$\widetilde{\mathbf{C}}_1 \succeq \mathbf{0}, \quad \widetilde{\mathbf{G}}_1 \succeq \mathbf{0}, \quad \widetilde{\mathbf{G}}_2^{\mathrm{T}}\,\widetilde{\mathbf{C}}_2^{-1}\,\widetilde{\mathbf{G}}_2 \succeq \mathbf{0}.$$

Hence, the SPRIM model preserves reciprocity, and thus can be more easily synthesized as an actual circuit.

6. NUMERICAL EXAMPLES

In this section, we present some numerical examples that illustrate the higher accuracy of the SPRIM reduced-order models vs. the PRIMA reduced-order models.

6.1 A PEEC Circuit

The first example is a circuit resulting from the so-called PEEC discretization [22] of an electromagnetic problem. The circuit is an RLC network consisting of 2100 capacitors, 172 inductors, 6990 inductive couplings, and a single resistive source that drives the circuit. The circuit is formulated as a 2-port. We compare the PRIMA and SPRIM models corresponding to the same dimension n of the underlying block Krylov subspace. The expansion point $s_0 = 2\pi \times 10^9$ was used. In Figure 1, we plot the absolute value of the $(2,1)$ component of the 2×2-matrix-valued transfer function over the frequency range of interest. The dimension $n = 120$ was sufficient for SPRIM to match the exact transfer function. The corresponding PRIMA model of the same dimension, however, has not yet converged to the exact transfer function in large parts of the frequency range of interest. Figure 1 clearly illustrates the better approximation properties of SPRIM due to matching of twice as many moments as PRIMA.

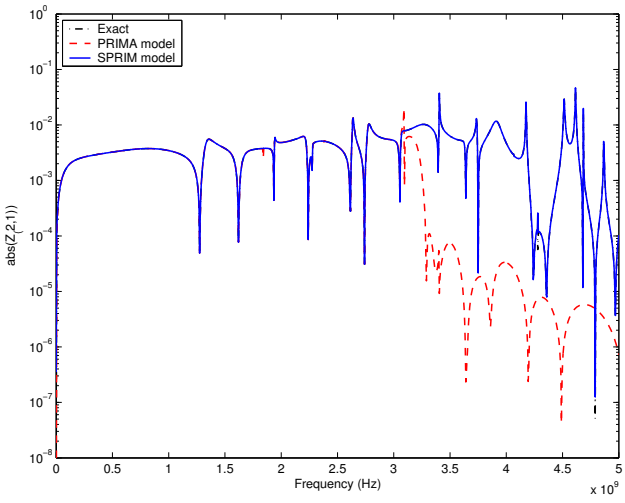

Figure 1: $|Z_{2,1}|$ for PEEC circuit

6.2 A Package Model

The second example is a 64-pin package model used for an RF integrated circuit. Only eight of the package pins carry signals, the rest being either unused or carrying supply voltages. The package is characterized as a 16-port component (8 exterior and 8 interior terminals). The package model is described by approximately 4000 circuit elements, resistors, capacitors, inductors, and inductive couplings. We again compare the PRIMA and SPRIM models corresponding to the same dimension n of the underlying block Krylov subspace. The expansion point $s_0 = 5\pi \times 10^9$ was used. In Figure 2, we plot the absolute value of one of the components of the 16×16-matrix-valued transfer function over the frequency range of interest. The state-space dimension $n = 80$ was sufficient for SPRIM to match the exact transfer function. The corresponding PRIMA model of the same dimension, however, does not match the exact transfer function very well near the high frequencies; see Figure 3.

6.3 A Mechanical System

Exploiting the equivalence (see, e.g., [18]) between RLC circuits and mechanical systems, both PRIMA and SPRIM can also be applied to reduced-order modeling of mechanical systems. Such systems arise for example in the modeling and simulation of MEMS devices. In Figure 4, we show a comparison of PRIMA and SPRIM for a finite-element model of a shaft. The expansion point $s_0 = \pi \times 10^3$ was used. The dimension $n = 15$ was sufficient for SPRIM to match the exact transfer function in the frequency range of interest. The corresponding PRIMA model of the same dimension, however, has not converged to the exact transfer function in large parts of the frequency range of interest. Figure 4 again illustrates the better approximation properties of SPRIM due to the matching of twice as many moments as PRIMA.

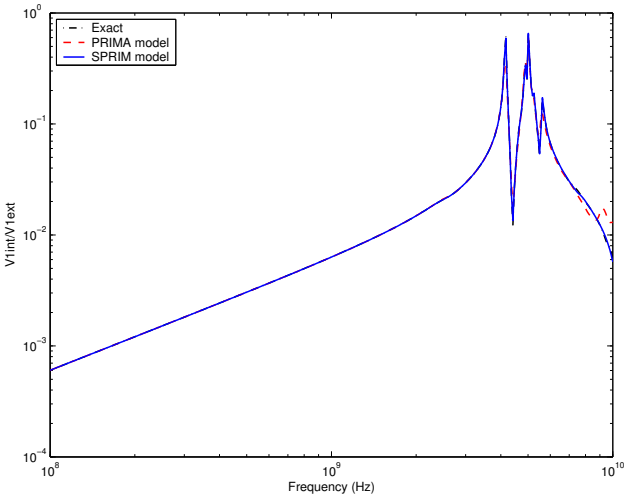

Figure 2: The package model

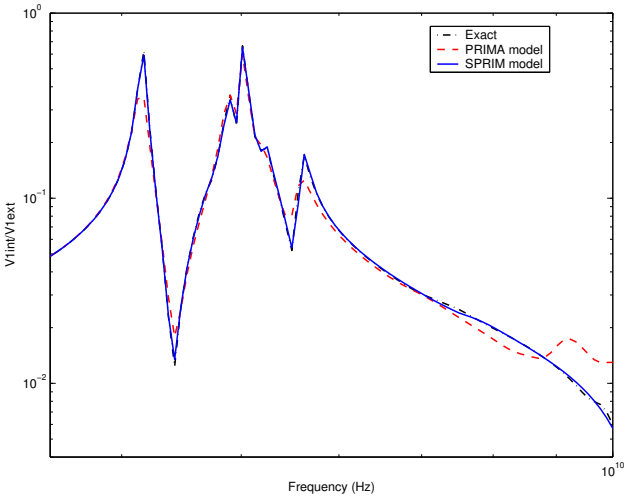

Figure 3: The package model, high frequencies

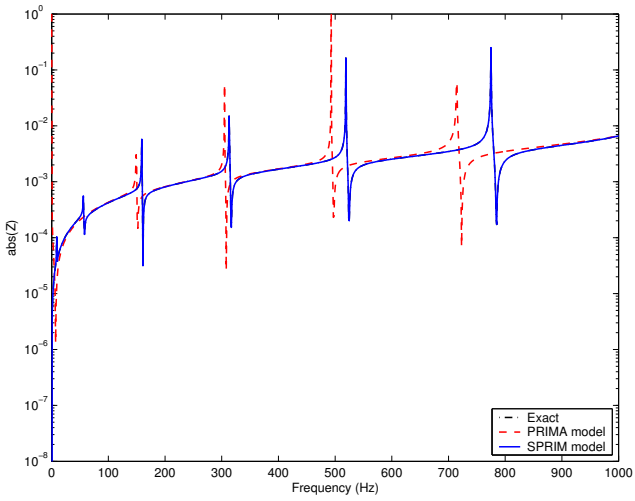

Figure 4: A mechanical system

7. CONCLUDING REMARKS

We have taken a fresh look at Krylov subspace-based projection techniques, such as PRIMA, for reduced-order modeling of large RLC circuits. We have shown that in order to obtain a PRIMA-like moment-matching property, one does not need to project onto a basis matrix for the underlying block Krylov subspace, but one can use any matrix whose column span contains that block Krylov subspace. Based on this insight, we proposed a novel projection technique, the SPRIM algorithm, that preserves all the crucial structures, such as passivity, reciprocity, and second-order form, of RLC circuits. In particular, since the SPRIM reduced-order models are reciprocal, they are easier to synthesize as actual RLC circuits; see, e.g., [2]. In addition, it also turns out that the SPRIM reduced-order models even match twice as many moments as the corresponding PRIMA models obtained with the same computational work. We presented numerical results that illustrate the higher accuracy of SPRIM vs. PRIMA.

8. REFERENCES

[1] J. I. Aliaga, D. L. Boley, R. W. Freund, and V. Hernández. A Lanczos-type method for multiple starting vectors. *Math. Comp.*, 69:1577–1601, 2000.

[2] B. D. O. Anderson and S. Vongpanitlerd. *Network Analysis and Synthesis*. Prentice-Hall, Englewood Cliffs, New Jersey, 1973.

[3] W. E. Arnoldi. The principle of minimized iterations in the solution of the matrix eigenvalue problem. *Quart. Appl. Math.*, 9:17–29, 1951.

[4] Z. Bai, P. Feldmann, and R. W. Freund. How to make theoretically passive reduced-order models passive in practice. In *Proc. IEEE 1998 Custom Integrated Circuits Conference*, pages 207–210, Piscataway, New Jersey, 1998. IEEE.

[5] G. A. Baker, Jr. and P. Graves-Morris. *Padé Approximants*. Cambridge University Press, New York, New York, second edition, 1996.

[6] T.-H. Chen, C. Luk, and C. C.-P. Chen. SuPREME: Substrate and power-delivery reluctance-enhanced macromodel evaluation. In *Technical Digest of the 2003 IEEE/ACM Int. Conf. on Computer-Aided Design*, pages 786–792, Los Alamitos, California, 2003. IEEE Computer Society Press.

[7] I. M. Elfadel and D. D. Ling. Zeros and passivity of Arnoldi-reduced-order models for interconnect networks. In *Proc. 34nd ACM/IEEE Design Automation Conference*, pages 28–33, New York, New York, 1997. ACM.

[8] P. Feldmann and R. W. Freund. Efficient linear circuit analysis by Padé approximation via the Lanczos process. In *Proceedings of EURO-DAC '94 with EURO-VHDL '94*, pages 170–175, Los Alamitos, California, 1994. IEEE Computer Society Press.

[9] P. Feldmann and R. W. Freund. Efficient linear circuit analysis by Padé approximation via the Lanczos process. *IEEE Trans. Computer-Aided Design*, 14:639–649, 1995.

[10] P. Feldmann and R. W. Freund. Reduced-order modeling of large linear subcircuits via a block Lanczos algorithm. In *Proc. 32nd ACM/IEEE Design Automation Conference*, pages 474–479, New York, New York, 1995. ACM.

[11] P. Feldmann and R. W. Freund. Interconnect-delay computation and signal-integrity verification using the sympvl algorithm. In *Proc. 1997 European Conference on Circuit Theory and Design*, pages 132–138, Los Alamitos, California, 1997. IEEE Computer Society Press.

[12] R. W. Freund. Passive reduced-order models for interconnect simulation and their computation via Krylov-subspace algorithms. In *Proc. 36th ACM/IEEE Design Automation Conference*, pages 195–200, New York, New York, 1999. ACM.

[13] R. W. Freund. Krylov-subspace methods for reduced-order modeling in circuit simulation. *J. Comput. Appl. Math.*, 123(1–2):395–421, 2000.

[14] R. W. Freund and P. Feldmann. Reduced-order modeling of large passive linear circuits by means of the SyPVL algorithm. In *Tech. Dig. 1996 IEEE/ACM International Conference on Computer-Aided Design*, pages 280–287, Los Alamitos, California, 1996. IEEE Computer Society Press.

[15] R. W. Freund and P. Feldmann. The SyMPVL algorithm and its applications to interconnect simulation. In *Proc. 1997 International Conference on Simulation of Semiconductor Processes and Devices*, pages 113–116, Piscataway, New Jersey, 1997. IEEE.

[16] R. W. Freund and P. Feldmann. Reduced-order modeling of large linear passive multi-terminal circuits using matrix-Padé approximation. In *Proc. Design, Automation and Test in Europe Conference 1998*, pages 530–537, Los Alamitos, California, 1998. IEEE Computer Society Press.

[17] C. Lanczos. An iteration method for the solution of the eigenvalue problem of linear differential and integral operators. *J. Res. Nat. Bur. Standards*, 45:255–282, 1950.

[18] R. Lozano, B. Brogliato, O. Egeland, and B. Maschke. *Dissipative Systems Analysis and Control*. Springer-Verlag, London, 2000.

[19] A. Odabasioglu. Provably passive RLC circuit reduction. M.S. thesis, Department of Electrical and Computer Engineering, Carnegie Mellon University, 1996.

[20] A. Odabasioglu, M. Celik, and L. T. Pileggi. PRIMA: passive reduced-order interconnect macromodeling algorithm. In *Tech. Dig. 1997 IEEE/ACM International Conference on Computer-Aided Design*, pages 58–65, Los Alamitos, California, 1997. IEEE Computer Society Press.

[21] L. T. Pillage and R. A. Rohrer. Asymptotic waveform evaluation for timing analysis. *IEEE Trans. Computer-Aided Design*, 9:352–366, 1990.

[22] A. E. Ruehli. Equivalent circuit models for three-dimensional multiconductor systems. *IEEE Trans. Microwave Theory Tech.*, 22:216–221, 1974.

[23] B. N. Sheehan. ENOR: model order reduction of RLC circuits using nodal equations for efficient factorization. In *Proc. 36th ACM/IEEE Design Automation Conference*, pages 17–21, New York, New York, 1999. ACM.

[24] L. M. Silveira, M. Kamon, I. Elfadel, and J. White. A coordinate-transformed Arnoldi algorithm for generating guaranteed stable reduced-order models of RLC circuits. In *Tech. Dig. 1996 IEEE/ACM International Conference on Computer-Aided Design*, pages 288–294, Los Alamitos, California, 1996. IEEE Computer Society Press.

[25] T.-J. Su and R. R. Craig, Jr. Model reduction and control of flexible structures using Krylov vectors. *J. Guidance Control Dynamics*, 14:260–267, 1991.

[26] M. R. Wohlers. *Lumped and Distributed Passive Networks*. Academic Press, New York, New York, 1969.

[27] H. Zheng, B. Krauter, M. Beattie, and L. Pileggi. Window-based susceptance models for large-scale RLC circuit analyses. In *Proc. 2002 Design, Automation and Test in Europe Conference*, Los Alamitos, California, 2002. IEEE Computer Society Press.

[28] H. Zheng and L. T. Pileggi. Robust and passive model order reduction for circuits containing susceptance elements. In *Technical Digest of the 2002 IEEE/ACM Int. Conf. on Computer-Aided Design*, pages 761–766, Los Alamitos, California, 2002. IEEE Computer Society Press.